

XMM

PHS Tools - EPIC Optical Loading

XMM-PS-TN-40 Issue draft

Written by: D. Lumb

November 16, 2000

1 Introduction

This note briefly describes issues related to one of the SSD-developed PHS tools, used to determine if the correct optical blocking filter has been chosen for a particular exposure.

The EPIC CCDs are highly sensitive to visible light, therefore if an astronomical target has a high optical-to-X-ray flux ratio, there is a possibility that the X-ray signal becomes contaminated by optical photons. The resulting analysis of data would be impeded in three ways:

1. Shot noise on the optically generated photoelectrons will degrade overall system noise, and hence the energy resolution. Spectral fitting will be inaccurate because the calibration files will assume narrower spectral line features
2. The energy scale will be incorrectly registered, because a nominally zero signal pixel will have a finite offset. For each optically generated photo-electron which is registered, the energy scale shifts about 3.6 eV. This is comparable with the accuracy with which we expect brightest emission line features could be centroided.
3. Excess signal and noise fluctuations can affect the detection efficiency as well, by disguising single pixel X-ray events as events split between pixels

To prevent this, the EPIC cameras include aluminised optical blocking filters, and also an internal “Offset Table” which is calculated before each exposure to subtract the dc level of light or other systematic zero shifts.

If these measures work perfectly, the above problems are minimised. However the use of a thick blocking filter capable of minimising light contamination for *all* scenarios would necessarily limit the softest X-ray response. EPIC has therefore decided to equip each camera with 4 separate filter selections, named THICK, MEDIUM, THIN and OPEN. It follows that it is necessary for the GO to select the filter which maximises the scientific return, by choosing the minimal optical blocking that is required for the target of interest. To aid in the evaluation of the selection, a ESTEC SSD-provided PHS tool is being produced to check the amount of light that contaminates a measurement. It is TBD if the tool will be supplied to GOs for the AO-1, certainly the summary of results will be provided as part of the Proposer’s Guide, together with a set of guidelines for use.

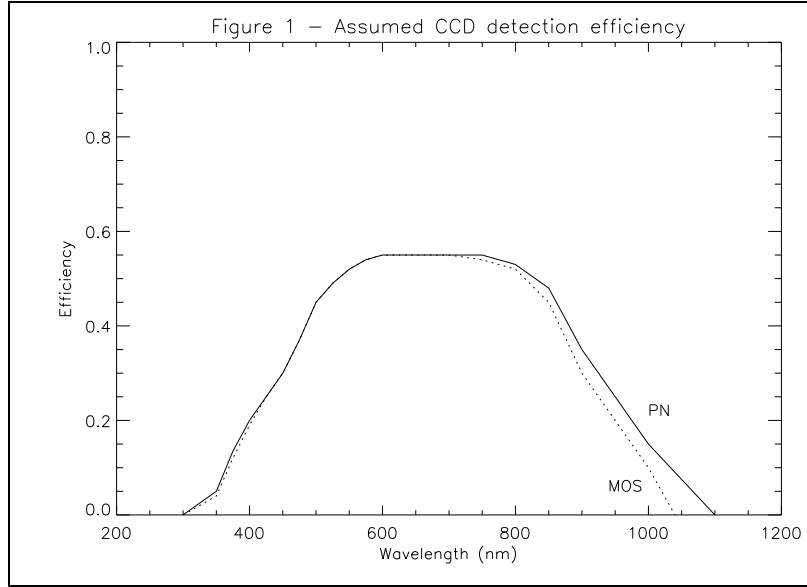
2 The Model

According to Zombeck’s Handbook of astrophysical data, the rough measure of flux from a A0 star of zero visible magnitude is about 10^3 photons per second per sq cm and per Angstrom. For sanity check purposes, then one could assume a telescope area 1800cm^2 , CCD efficiency 50% and a waveband of about 4000\AA . This leads to a total flux from the star of $4 \cdot 10^9$ photons/sec in an OPEN position, approximately focussed as the PSF.

The effective area of the telescopes for optical light will depend on the geometrical area, mirror reflectivity and (for the MOS cameras) blocking due to the RGA. Visible waveband reflectivity of gold is high, but a wavelength dependent distribution with a maximum value in the range 95 - 97% was not available. Given the large uncertainties with other terms in our model, we simply took the measured visible/UV geometric area measured at CSL as representative of the in-flight performance (1800 cm^2 for the PN camera, with a 45% throughput due to RGA blocking).

Figure 1 shows the assumed filter wavelength-dependent transmission coefficients, based on data from early engineering samples of filters. This data will require updating for the flight filters when available.

The key parameter for performance is actually the amount of light per pixel per CCD readout frame. There are some preliminary data showing that due to diffraction the optical light Point Spread Function may have a Half Energy Width of 30 arcsec, rather than a ≤ 20 arcsec response at X-ray wavelengths. However to be conservative, we assume that the fraction of light that is detected at a pixel in the peak of the PSF distribution will be 2% and 15% for the MOS and PN pixel sizes respectively.



Because the EPIC CCDs may operate in a wide range of readout modes, each presenting a different frame time collection, the basic model proceeds to calculate the optical loading per unit time, so that the exposure specific details may be abstracted.

The most problematic bright sources of optical loading will be point-like objects with visible magnitudes brighter than 10, therefore for most purposes we can estimate the loading based on simple stellar spectra. To perform this calculation we take simple black-body formulae as

$$f(\lambda) = \frac{6.73 \times 10^{10}}{T_e} 10^{-0.4m_b} P(\lambda, T_e) \quad (1)$$

photons $\text{cm}^{-2} \text{s}^{-1} \text{\AA}^{-1}$ where P is the Planck function

$$P = \frac{1.26 \times 10^{-8}}{\lambda^4 (\text{cm}) T_e^3} \frac{1}{e^{\frac{hc}{\lambda k T}} - 1} \quad (2)$$

where T_e is the effective temperature of the star, and m_b is the bolometric magnitude of the star, found from the bolometric colour correction appropriate to the stellar class.

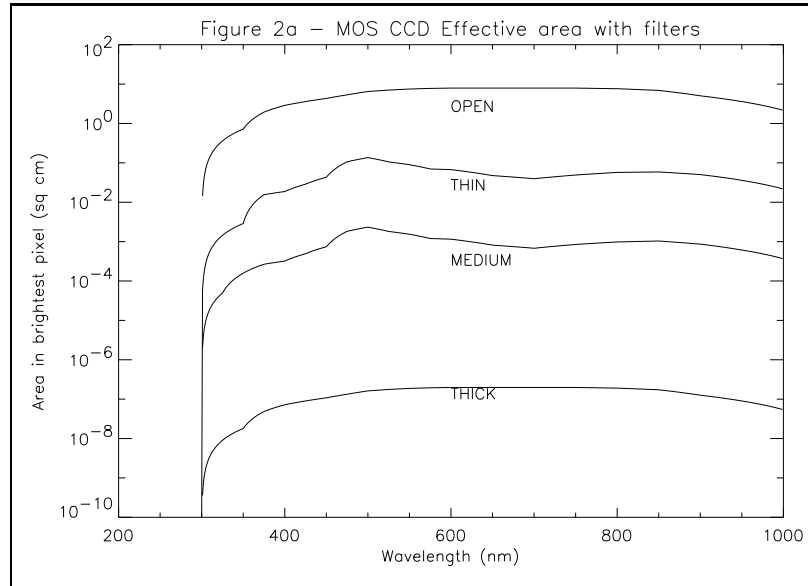
A look-up table will be produced from this model. It will contain for each CCD camera and filter combination a calculated value for each broad spectral type of the optical photons detected per second per pixel, for a visual magnitude of 0.

The observer would have to supply only the spectral type and visible magnitude, and the PHS tools will calculate the detected photons per pixel per CCD readout frame, based on the mode parameters of the readout and the magnitude conversion from the look-up table.

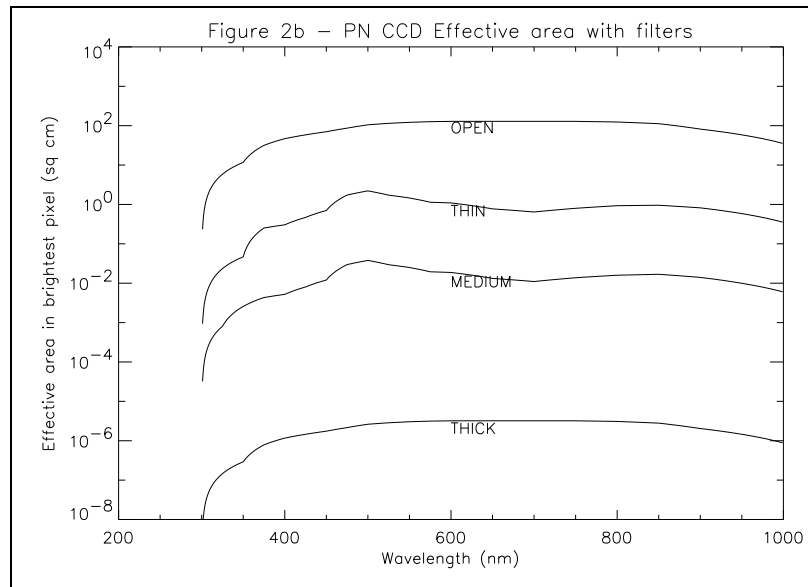
If the observer cannot provide a spectral type, we might assume a M-type (worst case value, and is representative of many galaxies that might be in any case be the target of some of those observations with unknown stellar type)

XMM Science Operations Team

Figures 2a and 2b shows the assumed CCD detection efficiencies for visible light. This is extrapolated from known astronomical CCD performance, but accounting for the fact that the EPIC CCDs have no anti-reflection coatings.



Note with the very deep PN camera depletion depths, the long wavelength detection efficiency is very high, leading to high sensitivity to late-type stars.



3 Results

Stellar Type	T_e (K)	BC (= $m_b - m_v$)	MOS				PN			
			THICK	MED	THIN	OPEN	THICK	MED	THIN	OPEN
M8	2660	-4.2	14.4	8.09e4	4.7e6	5.74e8	233	1.32e6	7.6e7	9.33e9
M0	3920	-1.2	2.0	1.18e4	6.85e5	8.11e7	32.8	1.93e5	1.11e7	1.32e9
K7	4160	-0.9	1.6	9.65e3	5.61e5	6.57e7	26.6	1.58e5	9.09e6	1.07e9
K0	5240	-0.19	0.98	6.0e3	3.48e5	3.93e7	15.9	9.78e4	5.64e6	6.38e8
G8	5490	-0.15	0.95	5.87e3	3.41e5	3.81e7	15.4	9.59e4	5.53e6	6.19e8
G0	5920	-0.06	0.88	5.46e3	3.17e5	3.5e7	14.2	8.91e4	5.14e6	5.69e8
F8	6200	-0.05	0.85	5.40e3	3.14e5	3.44e7	13.9	8.83e4	5.09e6	5.58e8
F0	7240	-0.08	0.82	5.30e3	3.07e5	3.29e7	13.3	8.62e4	4.97e6	5.34e8
A7	8190	-0.12	0.77	5.06e3	2.93e5	3.09e7	12.5	8.24e4	4.75e6	5.03e8
A0	10800	-0.40	0.72	4.83e3	2.79e5	2.86e7	11.6	7.85e4	4.52e6	4.66e8
B9	12400	-0.66	0.73	5.00e3	2.88e5	2.94e7	11.9	8.10e4	4.67e6	4.78e8
B0	30000	-3.17	0.11	7.82e3	4.47e5	4.46e7	18.0	1.26e5	7.24e6	7.24e8
O9	31900	-3.34	0.11	7.85e3	3.73e5	4.47e7	18.1	1.27e5	7.28e6	7.26e8

Pixel loading in photons per pixel per second

4 Operational Implications

The first interesting parameter we can derive from the above table is the maximum brightness allowed per point source if the calibration accuracy is not to be affected (i.e. assume the detected signal must be ≤ 1 electron per CCD frame time). The table is therefore recast below assuming the default operating modes of MOS = 2.6 secs FULL FRAME image mode, and PN = 0.07 secs FULL FRAME image mode. As a rough guide a source 1 - 2 magnitudes brighter could be handled with one of the EPIC window modes in each case. The units are in v magnitude.

Stellar Type	MOS				PN			
	THICK	MED	THIN	OPEN	THICK	MED	THIN	OPEN
M	3.9	13.3	17.7	22.9	3.0	12.4	16.8	22.0
K	1.55	11	15.4	20.8	0.67	10.1	14.5	19.7
G	1.0	10.5	14.9	20.3	0.08	9.6	14.0	19.2
F	0.86	10.4	14.8	20.2	-0.03	9.5	13.9	19.1
A	0.75	10.3	14.7	20.1	-0.14	9.4	13.8	19.0
B	1.14	10.8	15.2	20.6	0.25	9.9	14.3	19.5
O	1.14	10.8	15.2	20.6	0.25	9.9	14.3	19.5

An additional factor has also to be considered, particularly for the OPEN position. There is the existence of the zodiacal background which varies with ecliptic co-ordinate, and also the contribution from the galactic plane. The latter can be partially the diffuse Galactic UV light, but also the combination of confused point sources.

As a rule of thumb, in the Galactic plane, the number of unresolved stars per square arcsec is about $m_v 21.5$ equivalent. Thus in the PN camera the equivalent magnitude is 18.5 per pixel, decreasing to 21 at the galactic pole. In the MOS camera the equivalent numbers are 23.8 and 21.3. This stellar density may add to the overall noise on the pixels.

The zodiacal light appears as a truly diffuse source with G-type spectrum, varying from a magnitude of 23.4 to 21.6 per square arcsec, so the equivalent ranges per pixel are: 23.2 to 21.4 (MOS) and 20.4 to 18.6 (PN). At favourable galactic and ecliptic co-ordinates the EPIC cameras are able to utilise the OPEN position without degradation, but in general the unresolved light is comparable with the point source brightness limit.

If the observer's target is an extended source the magnitude must be entered as equivalent per point source. The conversion is probably not required to great accuracy, because one can expect that even the brighter nearby galaxies are classed as magnitudes 8 - 12 on spatial scales of several arcminutes, which corresponds to an equivalent magnitude per pixel of about 10 fainter.

Final considerations are more subtle practical ones. In the MOS camera the offset calculation is performed as averages along columns and rows. Therefore it may be possible that while the correct filter choice is made for the target of interest, brighter optical sources elsewhere in the same set of columns and/or rows may perturb the offset calculation with a negative energy delta applied at the interesting target, leading to incorrect energy assignment and event selection criteria again. (See for example technical note XMM-PS-TN-17 on the XMM SOC webpage http://astro.estec.esa.nl/XMM/tech/socdoc_top.html).

More generally the preceding analysis assumes no stray light in the form of earth and moon limb, or Solar system objects at close to the viewing constraints, nor stray light from pinholes in the instrument and spacecraft structure, poorly baffled filterwheel paths etc. etc.. As with the conservative margins adopted in the above calculations, we can only await actual measurements in-orbit before confirming these performance data.